Low-temperature thermal conductivity of amorphous silica

Mitra Dutta and Howard E. Jackson
Department of Physics, University of Cincinnati, Cincinnati, Ohio 45221
(Received 8 December 1980)

In order to understand the importance and limitations of the role of low-temperature thermal-conductivity data in understanding amorphous glasses, we have used the two-level tunneling-state model to generate fits to such data. A variety of densities of states have been utilized, including the forms previously suggested to explain specific-heat, ultrasonic-attenuation, and thermal-conductivity data. We find that the low-temperature (<3.5 K) fits to the data can be generated with all of the different forms of the density of states considered. In the intermediate temperature region (3.5–15 K) where there is a plateau, a variation in the strengths of the two different scattering processes, resonant and relaxation scattering processes, generates the various shapes seen in the thermal-conductivity data of different amorphous materials. With the strengths used for the best fit, we calculate the value of the coupling constant γ to be in accord with ultrasonic-phonon-echo experiments. The high-temperature thermal conductivity, above the plateau, requires a gentle tailing off in the density of states. Finally, an equally good fit to the complete thermal-conductivity curve can be generated with both a nearly constant density of states and a density of states which has a quadratic energy dependence.

INTRODUCTION

That amorphous materials form a distinct and different class of materials is seen, in the case of amorphous insulators, in the anomalies in the specific heat,[1,2] thermal conductivity,[1,2] attenuation and dispersion in the velocities of sound and ultrasound,[3] and in the existence of phonon echoes.[4] There exist a number of theoretical models which attempt to explain these anomalies, of which the two-level tunneling-state model due to Anderson, Halperin, and Varma[5] and independently Phillips,[6] has been the most successful. These two-level states, formed by the tunneling of entities in an asymmetric potential well, are considered intrinsic to the amorphous material. They contribute to the excess specific heat, scatter thermal and acoustic phonons, and produce the anomalies seen in experiment. The presence of the two-level tunneling states is embodied in two factors: the density of such two-level states, and the coupling constant γ which gives a measure of the coupling strength between the phonons and the two-level states. The coupling constant γ has been measured from phonon-echo experiments, whereas the product of the two factors, the density of states and γ, is determined from the specific-heat data and phonon scattering experiments, such as thermal-conductivity or ultrasonic-attenuation measurements. The two-level systems give rise to two distinct and important scattering mechanisms which are not present in pure crystalline materials. In an attempt to understand the behavior and importance of the two dominant phonon scattering mechanisms in different temperature ranges, we have studied the fit to the thermal-conductivity data of fused silica with several different forms of the density of states of these two-level systems.

The thermal conductivity K, is given by

$$K=\tfrac{1}{3}\sum_i \int_0^{\omega_{i,\max}} d\omega\, C_i(\omega) v_i l_i(\omega)\,, \tag{1}$$

where $C_i(\omega)$ is the specific-heat contribution of phonons of frequency ω and polarization i, and v_i and $l_i(\omega)$ are the velocity and total mean free path, respectively. We have assumed a tunneling-state model where the two-level systems are scattering the phonons. We have followed Smith, Anthony, and Anderson,[7] in taking the form of the total mean free path,

$$l_i = l_{\min} + (l_{\max}^{-1} + l_{i,\mathrm{res}}^{-1} + l_{i,\mathrm{rel}}^{-1})^{-1}\,, \tag{2}$$

where $l_{i,\mathrm{res}}$ and $l_{i,\mathrm{rel}}$ are the mean free paths due to the resonant and relaxation processes, respectively. Specifically, we have used $l_{\min}=1.5\times10^{-7}$ cm and $l_{\max}=3$ cm, where $l_{\max}$ is roughly the length of the sample. In Fig. 1 is displayed the thermal conductivity of a number of different amorphous insulators, all of which show essentially the same characteristic temperature dependence. We can analyze the thermal-conductivity data by considering three regions: (1) the low-temperature region (<3.5 K) where the temperature dependence is T^{δ}, where $\delta\cong1.8$, (2) the intermediate temperature region, the region where there is a plateau in the thermal-conductivity curve (~3.5–~15 K), and (3) the high-temperature region, that is beyond the plateau up to room temperature.

Following comments in Sec. I on the varieties of densities of states, some of which have been proposed previously to fit the experimental data, we discuss each of these temperature regions separately below in Secs. II, III, and IV. Finally,

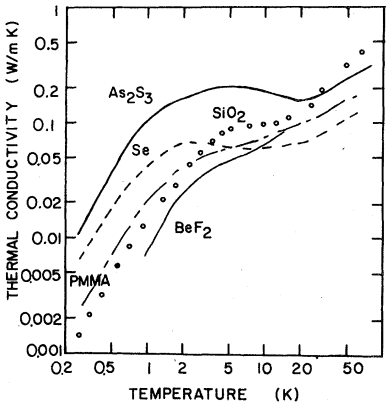

FIG. 1. Low-temperature thermal conductivity of some amorphous insulators. Data for SiO_2 is from Ref. 7, As_2S_3 and BeF_2 from Ref. 10, Se from Ref. 1 and polymethylmethacrylate (PMMA) from Ref. 2.

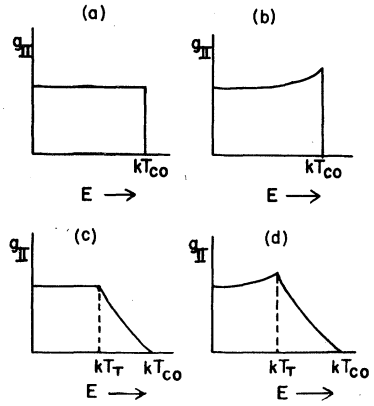

FIG. 2. Forms of some two-level density of states, g_{II}: (a) a nearly constant density of states with a sharp cutoff at an energy $E_{max}=kT_{co}$, (b) a density of states varying with energy and a sharp cutoff at $E_{max}=kT_{co}$, (c) a nearly constant density of states to $E=kT_T$ followed by decrease according to Eq. (6), and (d) an energy-dependent density of states to $E=kT_T$ followed by a decrease according to Eq. (6).

we remark on some considerations not fully explored here, in Sec. V, and present our conclusions.

I. VARIETIES OF DENSITIES OF STATES

From Eq. (1) we can see that a measurement of the thermal conductivity K is sensitive to the form of the density of states of the two-level systems, which are the dominant scatterers in amorphous insulators. We have studied a variety of different forms for the density of states in our attempt to fit the experimental data. We shall label the various forms of the density of states *a*, *b*, *c*, *d*, and numerical variations in a single form, for instance, by *b*-1, *b*-2, *b*-3. We have sketched each basic form in Fig. 2.

Figure 2(a) shows a constant density of states with a sharp cutoff at an energy E_{max}, equivalent to a cutoff temperature T_{co}. Figure 2(b) shows a density of states with an energy dependence or dispersion, and again with a sharp cutoff at $E_{max}=kT_{co}$. One of the main energy dispersive forms that we have considered is (form *b*-1),

$$\eta(E)P(E)=\begin{cases} P_m\left(\frac{E}{kT_N}\right)^{0.3}+P_n\left(\frac{E}{kT_N}\right)^{3.3} & \text{for } E<E_{max} \\ 0 \quad \text{for } E>E_{max}, \end{cases} \tag{3}$$

where $\eta(E)=\frac{1}{2}\ln(4\tau_{max}/\tau_{min})$, $P_m=1.04\times10^{33}$ erg^{-1}cm^{-3}, $P_n=9.8\times10^{29}$ erg^{-1}cm^{-3} following Smith *et al.*[7] The product[8] $\eta(E)P(E)$ is the total number of two-level systems, all of which contribute to the specific heat, while $P(E)$ are the more strongly-coupled states that scatter phonons and hence determine the thermal conductivity. We have also considered (form *b*-2),

$$\eta(E)P(E)=\begin{cases} P_m[1+a(E/kT_N)^2] & \text{for } E<E_{max} \\ 0 \quad \text{for } E>E_{max} \end{cases} \tag{4}$$

where $P_m=8.42\times10^{32}$ erg^{-1}cm^{-3}, $a=0.032$ following Stephens,[2] and (form *b*-3), $P_m=7.8\times10^{32}$ erg^{-1}cm^{-3}, $a=0.025$ following Hunklinger and Arnold.[3] $T_N=1$ K is a convenient normalization temperature in all three cases. We can set the second term of the density of states of form *b*-1 equal to zero:

$$\eta(E)P(E)=P_m(E/kT_N)^{0.3} \quad \text{for } E<E_{max}. \tag{5}$$

This is, in fact, the form we have used when we have considered a nearly constant density of states of the form shown in Fig. 2(a) (form *a*). In Fig. 2(c), we display a nearly constant density of states again, but instead of a sharp cutoff at E_{max}, we have, after a certain energy kT_T, a decrease in the density of states given by

$$P(E)=\frac{P_T}{(E/kT_N)^b} \quad \text{for } E>kP_T \tag{6}$$

where we have used a value of $P_T=3.97\times10^{33}$ erg^{-1}cm^{-3} and $b=0.3$ (form *c*). Another useful form (form *d*) is an energy dependence until $E=kT_T$ as in form *b*, and then the tail as above. This is sketched in Fig. 2(d). Now, let us look at each of the regions of the thermal conductivity curve in detail.

II. THE LOW-TEMPERATURE REGION

The resonant mean free path, due to the resonant interaction of phonons and the two-level systems, is given by[7]

$$l_{i,\mathrm{res}}^{-1} = \left(\frac{2\gamma^2}{\rho v^2}\right)_i \left(\frac{\pi}{2\hbar v_i}\right) E \tanh\left(\frac{E}{2kT}\right) P(E), \qquad (7)$$

where γ is the coupling constant and ρ is the mass density. At low temperatures (< 3.5 K), the resonant mean free path is the only one that is important. In Fig. 3, we display thermal-conductivity curves generated with different factors in front of Eq. (7), i.e., the l_{res}^{-1} has been multiplied by a factor which in case (a) is 0.5, in (b) is 0.75, in (c) is 1, and in (d) is 1.5. Figure 3 shows clearly that the low-temperature region is resonant dominated, and very sensitive indeed to the value of the resonant term. An increase in l_{res}^{-1} causes the thermal conductivity to decrease by the same factor. If we were using a constant density of states, we would get a T^2 dependence for the thermal conductivity, as has been predicted from theory. This can, in fact, be seen from the thermal-conductivity integral, in which l_{res}^{-1} is present alone, on applying the low-temperature limit. On using form *a* for the density of states, a thermal conductivity varying as $T^{1.8}$ as seen in experiment is obtained. We have compared the thermal conductivity obtained when one uses form *a* and form *b*-1 of the density of states. We find no difference at all at low temperatures. At low temperatures, the energy-dependent term simply does not matter. The low-temperature fit determines the coefficient in the density of states, which in our case was found to be $P_m = 7.34\times10^{32}$ erg^{-1} cm^{-3}, a somewhat smaller number than the 1.04×10^{33} erg^{-1} cm^{-3} found by Smith *et al.*[7]

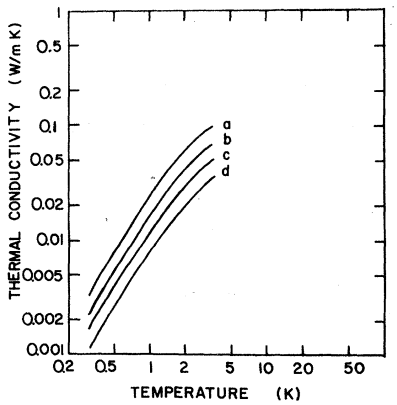

FIG. 3. Low-temperature thermal-conductivity curves generated with different values for the coefficient in front of Eq. (7), i.e., in the l_{res}^{-1} term. The values are in (a) 0.5, (b) 0.75, (c) 1, and (d) 1.5.

III. THE PLATEAU REGION

The next distinct temperature region we consider is the plateau region. We have attempted to generate the plateau in the thermal-conductivity data with just a resonant term included in the thermal-conductivity integral. We find that no fit is possible. One can see that directly from the integral. In the low-temperature limit, the temperature varies as $T^{1.8}$; in the high-temperature limit, the temperature dependence is T. Thus, the resonant term is not sufficient by itself to produce the plateau. Therefore, in this intermediate-temperature region, the relaxation processes must also start to contribute to the total mean free path.

From Hunklinger and Arnold,[3] we have τ^{-1}, the inverse lifetime of an individual two-level system,

$$\tau^{-1} = \left(\frac{M_i^2}{v_i^5} + \frac{2M_t^2}{v_t^5}\right) \frac{E^3}{2\pi\rho\hbar^4} \coth\frac{E}{2kT}. \qquad (8)$$

The coupling parameters M and D of Hunklinger and Arnold[3] reduce to $\gamma(\Delta/E)$ and $2\gamma(\Delta/E)$ on making the usual assumption that the dominant coupling of the phonons to the tunneling states is through a modulation of E. Here Δ is the overlap energy. With this,

$$\tau^{-1} = \sum_i \left(\frac{2\gamma^2}{\rho v_i}\right)_i \frac{\Delta^2 E}{4\pi v_i^3 \hbar^4} \coth\left(\frac{E}{2kT}\right). \qquad (9)$$

The inverse mean free path due to interaction between phonons and two-level system in a relaxation process is[3]

$$l_{\mathrm{rel}}^{-1} = \frac{ND^2}{\rho v^3} \frac{e^{E/kT}}{kT(1+e^{E/kT})^2} \frac{\omega^2\tau}{1+\omega^2\tau^2}, \qquad (10)$$

where N, the total number of two-level systems is

$$N = \int_0^{E_{\max}} \int_{\tau_{\min}}^{\tau_{\max}} P(E,\tau)\, d\tau\, dE \qquad (11)$$

and

$$P(E,\tau) = \frac{P(E)}{2\tau(1-\tau_{\min}/\tau)^{1/2}} \qquad (12)$$

is the probability density of a two-level system having energy E and lifetime τ. Using Eqs. (10), (11), and (12), we have,

$$l_{i,\mathrm{rel}}^{-1}=\left(\frac{2\gamma^2}{\rho v^3}\right)_i \frac{1}{4kT}\int_0^{E_{\max}} dE\,P(E)\,\mathrm{sech}^2\left(\frac{E}{2kT}\right)\int_{\tau_{\min}}^{\tau_{\max}} d\tau\,\frac{\omega^2(1-\tau_{\min}/\tau)^{1/2}}{1+\omega^2\tau^2}\,. \tag{13}$$

Equation (13) may be integrated in the high-frequency limit $\omega\tau_{\max}\gg 1$ and with $P(E)=\overline{P}$ (a constant density of states), and substituting $\tau_{\max}^{-1}$ from Eq. (9) we obtain,[9]

$$l_{i,\mathrm{rel}}^{-1}=\frac{1}{12}\left(\frac{2\gamma^2}{\rho v^2}\right)_i\left(\frac{1}{\pi v_i\hbar^4}\right)\sum_j\left(\frac{2\gamma^2}{\rho v^2}\right)_j\left(\frac{kT}{v_j}\right)^3\overline{P}\int_0^{E_{\max}/kT}\frac{(E/kT)^3}{\sinh(E/kT)}\,d\left(\frac{E}{kT}\right)\,. \tag{14}$$

For the case of an energy-dependent density of two-level states $P(E)$ the integral becomes, following Hunklinger and Arnold,[3,10]

$$l_{i,\mathrm{rel}}^{-1}=\left(\frac{4\gamma^2}{\rho v^3}\right)_i\frac{1}{4kT}\int_0^{E_{\max}} dE\,P(E)\mathrm{sech}^2\left(\frac{E}{2kT}\right)\sum_j\frac{E^3}{2\pi\rho\hbar^4}\left(\frac{\gamma^2}{v^5}\right)_j\coth\left(\frac{E}{2kT}\right), \tag{15}$$

where we have used an average relaxation time for each tunneling-level energy. We have used Eq. (15) for the calculations that follow.

Using a density of states of form b-1 and $l_{\min}$, $l_{\max}$, and $E_{\max}$ of Ref. 7, we are able to generate a plateau region. However, the calculated values of the thermal conductivity in this region were smaller, 0.06 W/mK, than the experimental value of 0.09 W/mK.[7] We have tried adjusting (i) the cutoff $E_{\max}$ and (ii) the coefficient A in Al_{rel}^{-1} using the l_{res}^{-1} determined from the low-temperature fit previously. Curve a of Fig. 4, shows $A=0.7$ and $T_{\mathrm{co}}=38$ K, curve b of Fig. 4 shows $A=1$ and $T_{\mathrm{co}}=20$ K, and curve c of Fig. 4 shows $A=1$ and $T_{\mathrm{co}}=10$ K. Figure 4 demonstrates that only lower values of the thermal-conductivity values and not higher values, as required by the data in the plateau region, could be generated.

Let us consider, for the moment, a constant density of states in an effort to understand why we could not raise the plateau to the required value. The resonant rate is $\tau_{\mathrm{res}}^{-1}=\alpha T(E/kT)\overline{P}\tanh(E/2kT)$ and the relaxation rate is $\tau_{\mathrm{rel}}^{-1}=\beta T^3(E/kT)^3\overline{P}$, where α and β are the coefficients with the values of velocity, density, and coupling constant that appear in the expression for τ_{res}^{-1} and τ_{rel}^{-1}. The numerical values for α and β for fused silica are 3.78×10^{-31} and 1.09×10^{-33}, respectively. These are obtained on inserting the numerical values of the constants in Eqs. (7) and (14) where, of course, $\tau^{-1}=vl^{-1}$. Thus, α and β are numbers derived from experimentally measured data and are not freely adjustable parameters. The ratio $\beta/\alpha=2.88\times10^{-3}$ governs the relative dominance of the roles of τ_{res}^{-1} and τ_{rel}^{-1} in determining the conductivity data as a function of temperature. If one allows this ratio to vary in order to obtain the best fit to the thermal-conductivity data, the expression β/α is obtained which gives a coupling constant γ equal to that obtained from ultrasonic measurements. In the case where an energy dependence in the density of states is included, these numerical factors will be modified by the integration of the energy-dependent density of states, the modifying factor being the same in both the rates, τ_{res}^{-1} and τ_{rel}^{-1}. We show what happens to the plateau region in the thermal conductivity with different values of the ratio β/α with a density of states of form a and form b-1. Figure 5 curve a shows form a with $\beta/\alpha=2.88\times10^{-3}$, while Fig. 5, curve b, shows that the plateau disappears when the ratio β/α is made smaller, $\beta/\alpha=2.88\times10^{-4}$. Figure 6, curve a, shows form b-1 with $\beta/\alpha=2.88\times10^{-3}$, while Fig. 6, curve b, is the same density of states with $\beta/\alpha=2.88\times10^{-4}$. The plateau region disappears as β/α becomes smaller, indicating that with the given expressions for the two rates, one cannot decrease the relaxation scattering rate by an order of magnitude without washing out the

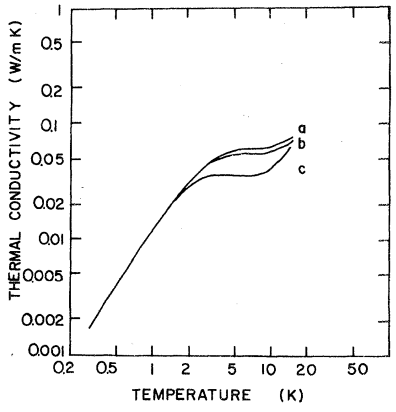

FIG. 4. Curves generated with Al_{rel}^{-1} using l_{res}^{-1} determined from the previous low-temperature fit. For (a) $A=0.7$ and $T_{\mathrm{co}}=38$ K, (b) $A=1$, $T_{\mathrm{co}}=20$ K, and (c) $A=1$ and $T_{\mathrm{co}}=10$ K. A density of states of form b-1 is used in all three cases.

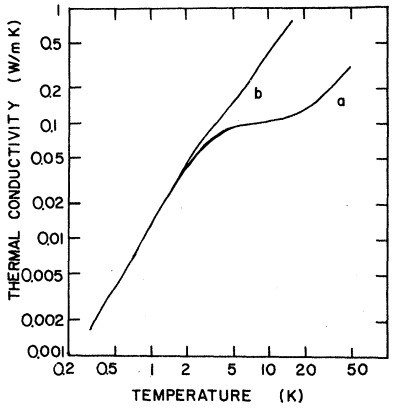

FIG. 5. Thermal conductivity generated with a constant density of states with the ratio β/α, the ratio of the relaxation rate to the resonant rate ($\tau_{\rm rel}^{-1}/\tau_{\rm res}^{-1}$), for the cases (a) 2.88×10^{-3} and (b) 2.88×10^{-4}.

plateau. This behavior shows quite clearly why we could not raise the plateau region to fit the experimental values, although we could lower it. Recall that the $\tau_{\rm res}^{-1}$ value has been previously fixed by the low-temperature fit of the thermal-conductivity data.

If the β/α ratio is increased, on the other hand, to $\beta/\alpha = 2.88\times10^{-2}$ for instance, a definite maximum and a minimum appear in the plateau, in the intermediate temperature region, due to the dominance of the relaxation process. This shape, as can be seen in Fig. 6, curve c, is reminiscent of the thermal conductivity measured for As_2S_3 and As_2Se_3.[2,11] The size of the β/α ratio has an important physical relevance as it gives a direct measure of the product $\gamma^2/\rho v^5$. Noting that the onset of the "peak" and "valley" in the thermal-conductivity curve occurs for a value of $\beta/\alpha \geq 9\times10^{-3}$ we have made an estimate of the coupling constant for As_2S_3 which is in agreement with the ultrasonic results of Claytor and Sladek[12] ($\sim\frac{1}{5}$ the γ for silica). Further, this ratio together with kT_T, the energy at which the density of states starts to decrease, governs the shape of the thermal-conductivity curve. A variety of shapes can be explained by the relative strengths of β and α, from a very weak plateau, to a strong peak and valley in the plateau region. Moreover, no new mechanism is required[11] to explain the maximum and minimum in the plateau.

We next attempt to fit the plateau region with a density of states form a and a change in the cutoff $T_{\rm co} = 15$ K. Figure 7 shows that we were able to fit the plateau region to the experimental data. We have therefore shown that while an energy-dependent density of states can generate a plateau in the thermal conductivity, the energy dependence is not essential as has been suggested[13,14] for the occurrence of the plateau. Further, a nearly constant density of states (form a), gives rise to the plateau in the correct place with respect to the experimental data.

The fact that we can fit the thermal-conductivity data with a constant density of states becomes interesting in light of the recent time-dependent specific-heat experiments of Loponen, Dynes, Narayanamurti, and Garno.[15] Their results show that the excess linear specific heat is due to two-level systems, but that the excess T^3 specific heat may arise from a different origin. The origin of the observed excess T^3 specific heat and the possible implications for the analysis of thermal-conduc-

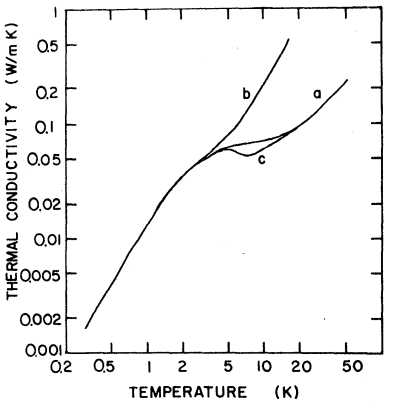

FIG. 6. Thermal conductivity generated with a density of states of form b-1 and β/α for (a) 2.88×10^{-3}, (b) 2.88×10^{-4}, and (c) 2.88×10^{-2}.

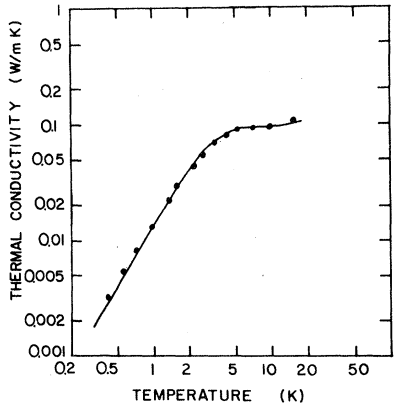

FIG. 7. Thermal conductivity in the plateau region generated with a nearly constant density of states. The points are the experimental data of Smith *et al.* (Ref. 7).

tivity data are not known. At this point, one should recall that, although an energy dependence may not be required to explain the larger than Debye T^3 term in the specific heat, it does appear necessary to explain, for instance, the velocity-dispersion results.[3,16]

IV. THE HIGH-TEMPERATURE REGION

In the high-temperature region (> 15 K), the slope of the thermal-conductivity curve above the plateau has a temperature dependence that is[7] $T^{1.15}$ over the range 15–60 K. Following Smith *et al.* we write the mean free path as

$$l_i = \begin{cases} l_{\min} + (l_{\max}^{-1} + l_{i,\mathrm{res}}^{-1} + l_{i,\mathrm{rel}}^{-1})^{-1} & \text{for } E < E_{\max} \\ l_{\min} & \text{for } E > E_{\max} . \end{cases}$$

Because $l_{\min}$ is not temperature dependent,[17] the thermal-conductivity integral has the temperature dependence of $C_i(\omega)$ integrated, which is $T^{2.65}$ with $\theta_T = 60$ and $\theta_L = 330$.[18] With the abrupt cutoff of the density of states at energy $E_{\max}$ the temperature arises from the integral over $C_i(\omega)$ and the resulting thermal conductivity $K \propto T^{2.65}$ is in sharp contrast to the observed $K \propto T^{1.15}$ dependence. The calculated values of the thermal conductivity, using an abrupt cutoff in the density of states (solid line), is compared to the experimental data (filled circles) in Fig. 8.

We have tried to fit the high-temperature (> 15 K) experimental data[7] with a decreasing density of states, or a "tail," beyond a certain energy kT_T (form *c* and form *d*). The results with a nearly constant density of states and a tail are shown in Fig. 9, curve *a*. The energy kT_T beyond which the density of states is characterized by a decrease according to Eq. (6),

$$P(E) = P_T \left(\frac{E}{kT_N}\right)^{-b} \quad \text{for } E > kT_T$$

with $T_T = 15$ K. Curve *b* of Fig. 9 shows the effect of form *d* where the energy dependence is of form *b*-1, with $T_T = 38$ K. Figure 10 shows again a density of states of form *d*, but now the energy dependence is of form *b*-3. The points are the experimental data points of Smith *et al.*[7] We would like to emphasize that this particular form of the tail is not unique, and that one could obtain the same fit with suitable adjustment of P_E

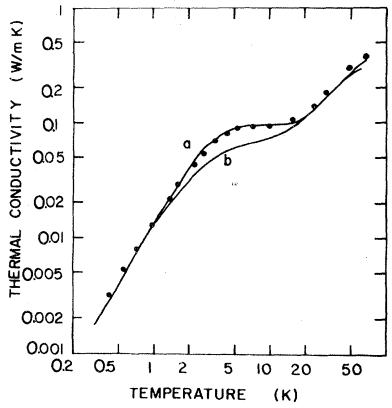

FIG. 9. Thermal conductivity generated in case (a) with a nearly constant density of states and a tail (form *c*), and (b) with a density of states of form *b*-1 and a tail. The points are the experimental data of Smith *et al.* (Ref. 7). See text for the physical significance of the parameters employed for this good fit and that of Fig. 10.

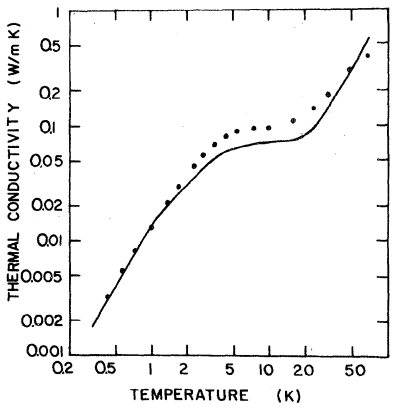

FIG. 8. Thermal conductivity generated with a density of states of form *b*-1 and a sharp cutoff. The points are the experimental data of Smith *et al.* (Ref. 7).

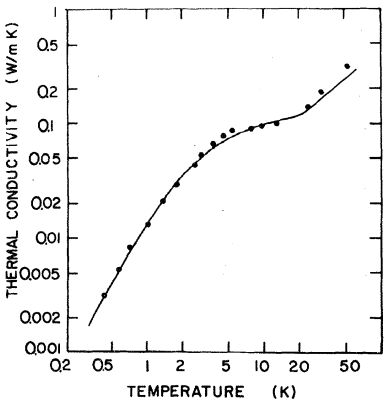

FIG. 10. Thermal conductivity generated with a density of states of form *b*-3 and a tail. The points are the experimental data of Smith *et al.* (Ref. 7). See text for the physical significance of the parameters employed for this good fit and that of Fig. 9.

with larger or smaller values of b. Furthermore, we would like to point out that changing the cutoff would require changes in P_E and b, as the contributions from the states above and below $E = kT_T$ change. Figures 9 and 10 show that the fits to the experimental data in the high-temperature region with the addition of the tail in the density of states, are very reasonable. On comparing the fit with and without the tail in the two-level density of states (see Figs. 8 and 9), it can be clearly seen that a tail in the density of states is essential to producing a fit to the experimental data.

V. OTHER CONSIDERATIONS

Let us consider some further ramifications of using these different forms of the density of states, particularly in considering data in addition to the thermal-conductivity data. We have, for instance, calculated the total number of states with form c, form b-1, and form b-3 of the density of states. With form c and $T_T = 15$ K, we arrive at a total number of states of 5.34×10^{19} cm^{-3} which is identical to that obtained from form b-3 and $T_{co} = 38$ K, 5.33×10^{19} cm^{-3}. The total number calculated from form b-1, is on the other hand, 2.08×10^{20} cm^{-3}, almost a factor of 4 larger. We also have looked at the low temperature ($\lesssim 2$ K) specific-heat data[7] and find our density of states, form c and form d, in good agreement. We have shown that an explicit fit to the thermal-conductivity data can be made with a nearly constant density of states, with a tail (Fig. 9, curve a). Nevertheless, an energy-dependent density of states is required to fit the ultrasonic attenuation and velocity dispersion data.[3,17] We have also shown that a good fit with a quadratic dependence in the density of states up to $E = kT_T$ and a tail beyond, is possible. However, a fit to the data could not be achieved with a cubic density of states. We would like to reiterate that the best fit achieved gave a coupling constant equal to that measured from the ultrasonic experiments, and a P_m, i.e., a coefficient to the density of states, consistent with the low-temperature specific-heat data.

CONCLUSION

In order to better understand the importance of the thermal-conductivity data to our physical understanding of amorphous insulators, and to understand the limitations of what may be learned from such information, we have generated a variety of fits to the thermal-conductivity data. We have seen that both a nearly constant density of states and a quadratic density of states generate equally good fits. Accordingly, one clear limitation emerges, that the fits do not allow one to specify a density of states uniquely. On the other hand, we have seen that a cubic energy dependence in the density of states cannot fit the data. Too strong an energy dependence although producing a plateau, does not yield the correct magnitude of the thermal conductivity in the intermediate temperature region. The low-temperature fit to the thermal conductivity specifies the coefficient P_m, the value of which is as expected, and agrees with the low-temperature specific-heat results. In the plateau region, the ratio of the relaxation to the resonant lifetimes β/α influences the magnitude, shape, and breakaway point from the $T^{1.8}$ dependence of the low-temperature region. This ratio is thus a signature of the particular form of the thermal-conductivity data: a definite plateau, weak plateau, or a peak and a valley in the plateau region. From this ratio, we have obtained not only the coupling constant for fused silica, which is in agreement with that obtained from ultrasonic experiments, but have also made an estimate of the coupling constant for As_2S_3 which is in reasonable agreement with ultrasonic experiments. Further, we have seen that given a particular density of states, the energy kT_T at which the density of states starts to decrease, determines the shape and the point at which the thermal-conductivity curve starts its upward trend again. Finally, the high-temperature slope cannot be fit with an abrupt cutoff in the density of states. Instead, it is essential to have a gentle tailing off in the density of states, a suggestion that is certainly physically reasonable.

ACKNOWLEDGMENTS

We acknowledge with pleasure useful conversations with Professor A.C. Anderson. The financial support of Research Corporation and of the University of Cincinnati Research Council is gratefully acknowledged.

[1] R. C. Zeller and R. O. Pohl, Phys. Rev. B 4, 2029 (1971).
[2] R. B. Stephens, Phys. Rev. B 8, 2896 (1973).
[3] S. Hunklinger and W. Arnold, in *Physical Acoustics*, edited by W. P. Mason and R. N. Thurston (Academic, New York, 1976), Vol. 12, p. 155.
[4] B. Golding and J. E. Graebner, Phys. Rev. Lett. 37, 852 (1976).
[5] P. W. Anderson, B. I. Halperin, and C. M. Varma, Philos. Mag. 25, 1 (1972).

[6]W. A. Phillips, J. Low Temp. Phys. 7, 351 (1972).
[7]T. L. Smith, P. J. Anthony, and A. C. Anderson, Phys. Rev. B 17, 4997 (1978).
[8]J. L. Black, Phys. Rev. B 17, 2740 (1978).
[9]The value of the integral over $d\tau$ in Eq. (13) reaches 95% of its asymptotic value at $\omega = 10^6$ so that in the temperature range of interest here, one is in the high-frequency limit. If one takes the limit of the integral of Eq. (15) as $E_{max} \rightarrow \infty$ (or $T \rightarrow 0$), Eq. (10) of Ref. 7 is recovered.
[10]One has a choice here of integrating over the energy dependence of $\tau_{min} = (\Delta/E)^2\tau$ or following Hunklinger and Arnold. Either approach gives equivalent results.
[11]A. J. Leadbetter, A. P. Jeapes, and C. G. Waterfield, J. Phys. (Paris) 38, 95 (1977).
[12]T. N. Claytor and R. J. Sladek, Phys. Rev. B 18, 5842 (1978).
[13]M. P. Zaitlin and A. C. Anderson, Phys. Status Solidi B 71, 323 (1975).
[14]D. P. Jones, N. Thomas, and W. A. Phillips, Philos. Mag. B 38, 271 (1978).
[15]M. T. Loponen, R. C. Dynes, V. Narayanamurti, and J. P. Garno, Phys. Rev. Lett. 45, 457 (1980).
[16]L. Piche, R. Maynard, S. Hunklinger, and J. Jäckle, Phys. Rev. Lett. 32, 1248 (1976); J. Jäckle, L. Piche, W. Arnold, and S. Hunklinger, J. Non-Cryst. Solids 20, 365 (1976).
[17]G. A. Slack, in *Advances in Research and Applications. Solid State Physics*, edited by H. Ehrenreich, F. Seitz, and D. Turnbull (Academic, New York, 1979), Vol. 34, p. 1.
[18]N. Bilir and W. A. Phillips, Philos. Mag. 32, 113 (1975).